The role of Ti^{3+} interstitials in TiO_2(110) reduction and oxidation

2009 J. Phys.: Condens. Matter 21 474224

(http://iopscience.iop.org/0953-8984/21/47/474224)

J. Phys.: Condens. Matter **22** (2010) 059801 (1pp) doi:10.1088/0953-8984/22/5/059801

Corrigendum

The role of Ti^{3+} interstitials in TiO_2(110) reduction and oxidation

Michael Bowker and Roger A Bennett

2009 *J. Phys.: Condens. Matter* **21** 474224

The authors have had an error in the description of the titanium sublattice of competing models for the (1 × 2) reconstructed TiO_2(110) surfaces brought to their attention. The sentence starting on the 4th line of page 3 should read 'This effectively places an added row Ti in an interstitial position either with horizontal (*ih*, Park model) or vertical (*iv*, Onishi–Iwasawa model) octahedral coordination (if one imagined an extension of the bulk).' The original manuscript has the assignment of the Ti positions in the models transposed, and we would like to apologise for any confusion caused.

J. Phys.: Condens. Matter **21** (2009) 474224 (9pp) doi:10.1088/0953-8984/21/47/474224

The role of Ti^{3+} interstitials in TiO_2(110) reduction and oxidation

Michael Bowker[1] **and Roger A Bennett**[2]

[1] Wolfson Nanoscience Laboratory, School of Chemistry, Cardiff University, Cardiff CF10 3AT, UK
[2] School of Chemistry, University of Reading, Reading RG6 6AF, UK

Received 18 May 2009, in final form 8 June 2009
Published 5 November 2009
Online at stacks.iop.org/JPhysCM/21/474224

Abstract
Here we describe results which teach us much about the mechanism of the reduction and oxidation of TiO_2(110) by the application of scanning tunnelling microscopy imaging at high temperatures. Titania reduces at high temperature by thermal oxygen loss to leave localized (i.e. Ti^{3+}) and delocalized electrons on the lattice Ti, and a reduced titania interstitial that diffuses into the bulk of the crystal. The interstitial titania can be recalled to the surface by treatment in very low pressures of oxygen, occurring at a significant rate even at 573 K. This re-oxidation occurs by re-growth of titania layers in a Volmer–Weber manner, by a repeating sequence in which in-growth of extra titania within the cross-linked (1 × 2) structure completes the (1 × 1) bulk termination. The next layer then initiates with the nucleation of points and strings which extend to form islands of cross-linked (1 × 2), which once again grow and fill in to reform the (1 × 1). This process continues in a cyclical manner to form many new layers of well-ordered titania. The details of the mechanism and kinetics of the process are considered.

M This article features online multimedia enhancements

(Some figures in this article are in colour only in the electronic version)

1. Introduction

Titania is an important material in all sorts of technological application, ranging from catalysts [1] to paints and optical coatings [2], from self-cleaning surfaces and photocatalysts [3] to anti-bacterial coatings or the structural interface in medical implants [4]. Many of these technologies depend crucially on the nature of the surface layers, and this partly explains the explosion of interest in recent years in the surface structure and properties of TiO_2 single crystals [5]. But titania is also of inherent scientific interest for a variety of reasons including it is reducibility, range of morphologies and particularly, as far as we are concerned, its surface structure and reactivity. Stoichiometric TiO_2 has four polymorphs: rutile, anatase, brookite and a recently discovered super-hard cotunnite structure [6]. The anatase phase is of principal interest in photoactive applications due to a direct bandgap of ∼3 eV. Anatase is often found as the dominant structure in high surface area powders, however, the most thermodynamically stable bulk structure under ambient conditions is rutile. Rutile TiO_2 is one of the few synthetic single crystals of oxides which are readily available which makes it a prime candidate for reproducible study. Fortunately it shows high electrical conductivity with relatively low levels of bulk reduction which makes it amenable to probing by surface science charged particle spectroscopies and it has proved ideal for scanning tunnelling microscopy (STM) studies.

The level of bulk reduction fundamentally influences the nature of non-stoichiometric rutile through the development of point and planar bulk defects and modified surface reconstructions and reactivity. The characterization of the bulk point defects in bulk rutile by materials scientists over the years conclusively pointed to titanium interstitials as being the dominant defect by far [7]. The interstitials are mobile in the bulk [8] via an interstitialcy diffusion mechanism (push out of a lattice Ti by an interstitial Ti which leaves a neighbouring Ti interstitial site also occupied). At high densities the interstitial point defects aggregate to form platelets of locally higher concentration of Ti within the bulk. These ultimately grow and aggregate to form crystallographic shear planes [9]. Given sufficient time at elevated temperature nearly stoichiometric rutile with crystallographic shear planes can self-assemble into homologous series of planar Magneli phases: Ti_nO_{2n-1} with $(4 < n < 10)$

based on {121} directed planes; and ($16 < n < \sim 37$) based on {132} planes [10–12]. Further stable reduced phases from Ti_4O_7, a crystal structure with promising electrical characteristics [13], to Ti_2O_3 can be formed as rutile is further reduced. Ti_2O_3 is a corundum structured pure Ti^{3+} phase which also appears as a reduced surface phase on near stoichiometric rutile surfaces treated in vacuum [14].

While the materials scientists have a clear description of the bulk properties, the surface chemistry community has had a very chequered history in describing the properties of the reduced surface. Undue prominence was initially given to the bulk oxygen vacancy model which has propagated over time despite the almost complete absence of experimental support for oxygen vacancies in the near surface region. This situation was markedly improved by Henderson [7] who employed isotopically labelled ^{18}O and ^{46}Ti in static secondary ion mass spectrometry to show that bulk-assisted re-oxidation of reduced surfaces was mediated by titanium cation diffusion and not by oxygen anions or vacancies. Direct visualization of this process was shown by Onishi and Iwasawa [14] who exposed a reduced surface at elevated temperature to O_2 and observed the growth of new surface layers. This demonstrates the mobility and reactivity of titanium interstitials in the subsurface region. By combining the SSIMS and STM techniques Li *et al* were able to quantify the oxygen uptake and to deduce a low temperature (<530 K) activation barrier of 0.82 eV/atom [15]. Above 530 K the rate of oxygen uptake began to drop and no longer followed Arrhenius behaviour. The rate of oxygen uptake was dependent upon the degree of non-stoichiometry with faster uptake on the most non-stoichiometric surfaces. Further *in situ* high temperature STM studies [16] quantified the growth rate of the surface (in contrast to isotopically labelled oxygen incorporation) and these data are detailed below. Oxygen vacancies (and OH groups that image similarly) have been identified by STM on the bridging row oxygen sites that are present on the (110) surface, although their removal does not restore the surface stoichiometry spectroscopically as the selvedge still contains many interstitials [17]. Their role in surface reactivity appears to be transient and they take no active part once saturated.

The focus of the work presented here is to show how the surface structure changes with increasing bulk reduction and how reduction and oxidation of the surface proceeds in detail. Essential to these findings are the use of repeated images (in the form of movies) which are obtained at HIGH temperature. *In situ* high temperature studies of oxide surfaces are relatively rare in the literature, due to the great problem of thermal drift which makes repeated imaging impossible in most STM systems. However, they provide an unprecedented view of the surface processes and enable characterization of minority structures and nanoscale kinetics.

2. Experimental details

The experiments were performed with an WA Technology variable temperature STM mounted in a single chamber with facilities for Ar^+ ion sputtering, LEED/RFA Auger (VG Scientific), temperature programmed desorption and gas dosing. Tips were prepared by electrochemical etching of W(97%)Re(3%) alloy wire of 0.2 mm diameter in KOH. A more detailed description of the apparatus may be found elsewhere [18]. The TiO_2(110) single crystals (PI KEM, UK) were prepared by repeated sputter (600 eV, 1000 K) and anneal (1200 K) cycles to produce crystals of various stoichiometries and indicated by their colour from light blue (nearly stoichiometric) to dark blue/black crystal (non-stoichiometric and showing small CSPs). Ca was seen to be the main impurity removed during cleaning (it produces a sharp c(2 × 6) LEED pattern [19]). During the initial preparation stages a (1 × 1) surface could be prepared by annealing at 1200 K (light blue crystals), however, with time this procedure produced predominantly the Ti_2O_3 type (1 × 2) termination on a blue crystal. After even more cycles of sputter/anneal treatments only the cross-linked (1 × 2) surface could be prepared (dark blue). While it is difficult to assess the level of reduction of the crystal we have observed some small features which we assign as precursors to CS plane formation. This indicates that at this stage the crystal has a stoichiometry of approximately TiO_{2-x}, $x < 10^{-3}$ [10]. Images take around 60 s to acquire and save and so the movies represent time lapse images of the surface. A linear background subtraction is employed which removes thermally induced vertical drift from the images. There is no compensation for lateral drift other than moving the tip slightly between images to maintain imaging of approximately the same area.

3. The effect of reduction of the surface structure of TiO_2(110)

Figure 1 shows a set of images of the titania surface taken over the prolonged use of a crystal in the UHV machine, which involves a range of thermal treatments, ion sputtering, oxidative treatments, as described above. Initially one sees a (1 × 1) phase on the clean surface, a structure which has been the subject of intense investigation, both experimental and theoretical [5], and continues to be so. It consists of alternating rows of oxygen and 5-fold coordinate Ti ions running in the ⟨001⟩ direction, and the bright rows which are imaged with positive sample bias are the Ti atoms, even though topologically they are well below the rows of bridging oxygen atoms. This is a good example where topography is inverted due to electronic structure effects [20]. Point defects are occasionally seen as bright features on the 'troughs' of the bridging oxygen, especially at room temperature or lower temperatures, and these may be oxygen vacancies or hydroxyl groups. At elevated temperature, as used here, hydroxyls are not stable. Upon reduction sometimes an intermediate (1 × 3) phase is seen, as shown in figure 1(b), though this is rarely reported and seems difficult to reproduce [21]. More commonly reported is the next phase—the (1 × 2), for which several models have been postulated [14], in figure 1(c) we show the Onishi and Iwasawa model which recent LEED-IV work suggests is correct [22, 23], although direct imaging by transmission electron microscopy of thin TiO_2 slices [24] is at odds with this work and supports an alternative structure proposed by Park [25]. Both of these structures basically

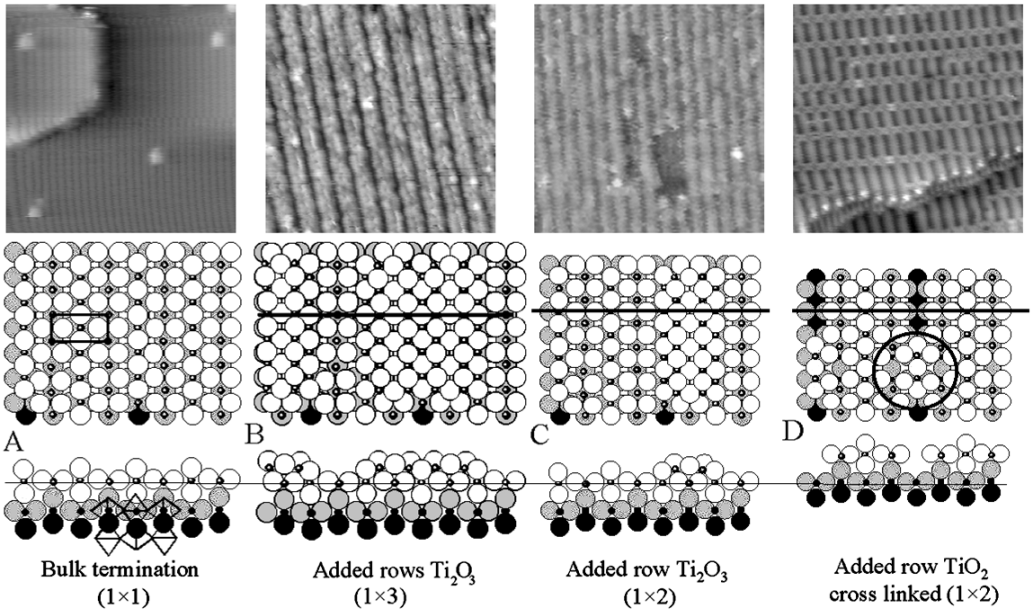

Figure 1. The surface structures seen on $TiO_2(110)$ during increasing bulk reduction of the crystal (from left to right). The upper panels are STM images with 20 nm scan size. The lower two panels are plans and elevations of the proposed surface structures.

consist of added rows of Ti_2O_3 stoichiometry lining up in the ⟨001⟩ direction and doubly spaced with respect to the underlying (1 × 1), the two models disagreeing on the registry to the underlying lattice by half a unit cell. This effectively places an added row Ti in an interstitial position either with horizontal (*ih*, Onishi–Iwasawa model) or vertical (*iv*, Park model) octahedral coordination (if one imagined an extension of the bulk). The *ih* and *iv* notation follows the work of Elliott and Bates [26] who surveyed a wide range of (1 × 2) reconstructions by DFT [27]. Recent combined DFT + U and experimental work show that Ti adsorbs preferentially on the *ih* position of the clean surface [28], with *ih* and *iv* only becoming degenerate several layers below the surface [29]. Upon further bulk reduction the structure shown in figure 1(d) is obtained, known as the cross-linked (1 × 2), which appears with higher z contrast to the usual Ti_2O_3 terminated (1 × 2) in STM and with linking structures periodically between (1 × 2 rows). These cross-links are strongly correlated across rows and so order to form a (n × 2) with n ∼ 11 or 12. Although the two types of (1 × 2) lines appear superficially similar they are quite different being ∼2.8 Å high for the cross-linked surface versus ∼1.3 Å for the simple (1 × 2) and they have notably different surface reactivity, as discussed in more detail elsewhere [30]. Upon more severe reduction we begin to see new structures appear on the surface, these are crystallographic shear planes (CSPs), which propagate from the bulk to the surface and manifest themselves at the surface as diagonal lines. As the crystal reduces further, beautiful, long straight lines appear, and as their density increases they become ordered in periodic striped arrangements. The lines are the surface truncation of a planar structure in the bulk, and appear as a pair of step edges where the crystal between the planes is crystallographically sheared by an $\frac{1}{2}\langle 0\bar{1}1\rangle$ displacement. These stripe structures may be alternate up–down steps which do not change the planar surface orientation or a long sequence of up or down steps

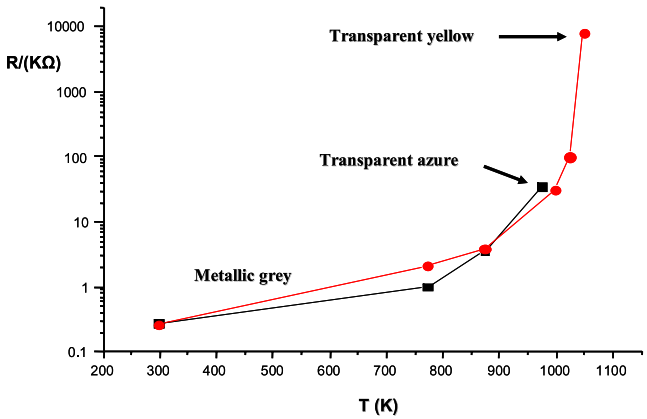

Figure 2. The resistance of two heavily UHV-reduced $TiO_2(110)$ crystals a function of annealing temperature in air (1 h at temperature).

which lead to the re-orientation of the surface and faceting. At this stage the crystal is highly reduced (estimated TiO_{2-x}, x is $\sim 10^{-3}$), is black in colour and comprises macroscopic rumpling of the surface due to the facets which becomes visible to the naked eye.

In her review [5] and elsewhere [31] Diebold reports the colours and electrical conductivity of some TiO_2 crystals treated in different ways to induce bulk reduction. Figure 2 shows the effect of heating two crystals (removed from UHV after considerable reduction, resulting in extensive CSP formation, as described above) in terms of conductivity and colour after such air treatment. Clearly conductivity is very high on removal from the UHV system, and the crystals appear to return close to their original condition after heating in air at 1050 K for 1 h. Unfortunately we have never placed one of these air re-oxidized samples back in UHV to examine whether the surface structure is good and imageable by STM. That would be an interesting exercise.

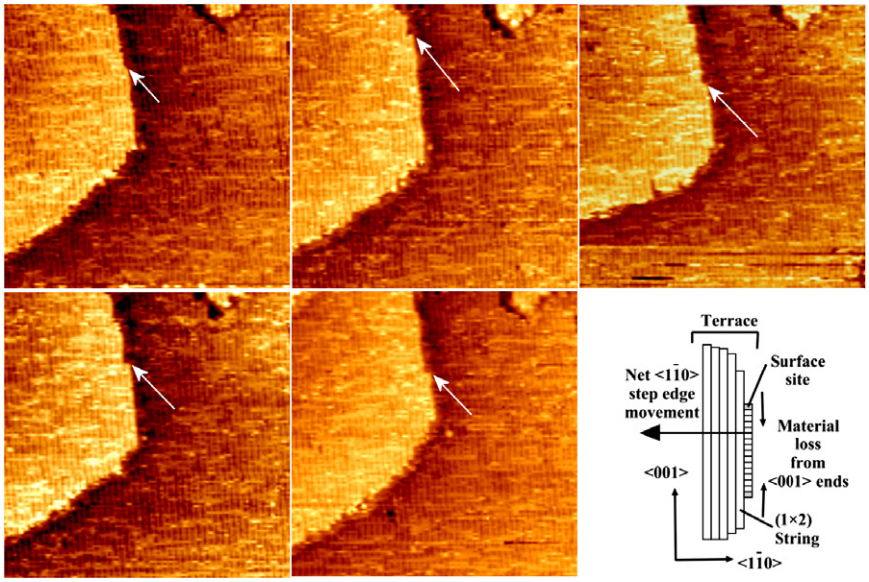

Figure 3. High temperature (1000 K) UHV STM image sequence (from left to right at $t = 0$, 6, 13, 21 and 32 min) of the cr-(1 × 2) surface, each image is 50 nm^2. The ends of the cross-linked rows retreat slowly which is especially noticeable at a step edge where the ends appear as kinks. These retreating kink sites are highlighted with an arrow. The picture illustrates the morphology of the step edge movement.

4. How reduction occurs

Studies of the reduction of the titania surface are very few, so many questions remain about exactly how this process occurs. We can imagine at least two processes, one driven simply by high temperature annealing in UHV leading to thermal desorption of oxygen, the other is through Ar^+ ion sputtering during cleaning which preferentially removes oxygen. However, sputtering with O^+ ions [28] also leads to the same reduced surface and so the elevated temperatures required to re-order the damaged surface are probably the dominant mechanism. The crystals are suitably electrically conducting such that charge is conserved so departing oxygen ions give up their electrons to the crystal (equation (1)).

$$TiO_{2(s)} \rightarrow Ti^{n+}_{(i)} + O_{2(g)} + ne^-. \quad (1)$$

There is much current interest in determining the oxidation states of the crystal that arise from the injection of electrons. Traditional density functional (DFT) calculations predicted delocalized electrons across the Ti ions in the due to surface or bulk defects with the crystal [32]. In recent work we have used the experimental study of self-doped (i.e. sub monolayer Ti added to a stoichiometric surface) titania films and single crystals to characterize the electronic properties of the Ti adatom and the reduced surface [28]. These well controlled systems allow systematic study and benchmarked companion DFT + U calculations to be performed to interpret the experiments and understand how the charge is distributed around the defect. The DFT+U calculations have an empirical element through the selection of the value for U to correct for on-site Coulomb interaction to describe reduced Ti ions. In this work, using the PW91 exchange correlation functional [33], large values of $U = 6$ eV strongly localize the extra electrons on the adatom and surface Ti, whereas $U = 0$ delocalizes the extra electrons through the surface region, and intermediate values yield a situation between these two extremes. It is the last case, specifically with $U = 3$ eV, that gives the best agreement with the spectroscopy of the gap states induced by the adsorbed adatom [28]. Calculations of oxygen vacancies in the (110) surface [34], which also reduce surface Ti, and latter calculations with the B3LYP functional (a different form of on-site correction) [35] also localize the Ti 3d states. The new insight afforded by these methods shows that the charge is strongly correlated to the site of the point defect (surface Ti, oxygen vacancy and Ti interstitial) and not delocalized over the bulk. The reduced Ti is generally in the 3+ state (although we find a significant population of Ti adatoms to be in 2+ state [28]).

We have observed the thermal reduction of a reconstructed surface by following the rate of (1 × 2) reconstructed string retreat at 1000 K. As O_2 is lost from the surface the remaining Ti is left behind, as described above probably as Ti^{3+} ions, and at elevated temperatures it disappears into the bulk, and so the steps retreat (figure 3). The rate of (1 × 2) string retreat at 1000 K yields an activation barrier of ∼3 eV for an assumed prefactor of 10^{13} s^{-1} (±0.2 eV for order of magnitude changes in the prefactor). This compares favourably with the reverse reaction (on the unreconstructed surface) which is predicted in DFT calculations to be exothermic for the dissociative binding of O_2 to surface excess Ti by ∼4 eV [17]. We have furthermore experimentally characterized the rate of dissolution of Ti into a stoichiometric surface. By depositing submonolayer Ti on a stoichiometric surface we mimic the Ti left behind by thermal or ion bombardment removal of oxygen. We find the as adsorbed Ti is in the 2+ oxidation state [28] which rapidly changes to 3+ upon thermal annealing. We then follow the dissolution by monitoring changes to the intensity of Ti $2p_{3/2}$ core level shifted components as a function of time and temperature yielding an activation barrier of 0.44±0.06 eV

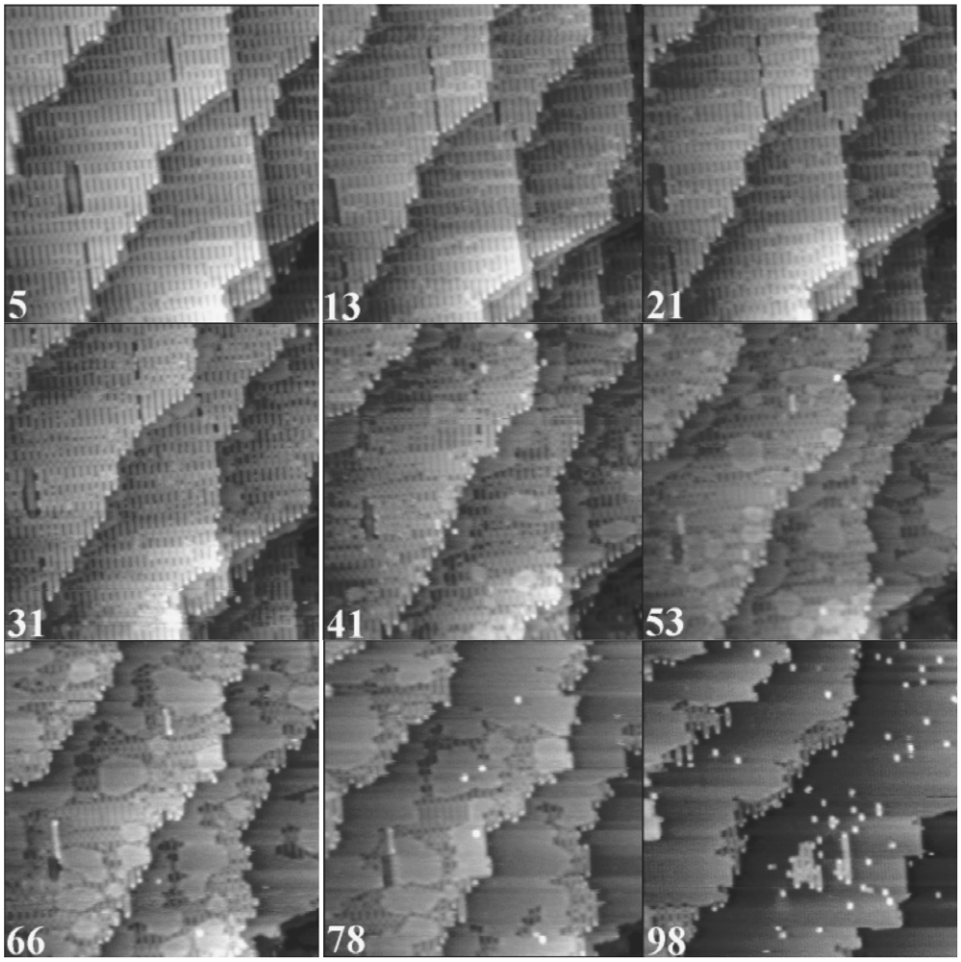

Figure 4. A series of 'snapshots' images of the initially cross-linked (1 × 2) surface during oxygen dosing at 673 K; the image sizes are 50 nm. The oxygen pressure during the imaging was 2×10^{-7} mbar up to frame 21, then 3.8×10^{-7} to frame 31, then 5.8×10^{-7} thereafter. The images are taken from movie associated with this paper as supplementary material (available at stacks.iop.org/JPhysCM/21/474224); the movies at other temperatures are also given elsewhere [16]. The images show the growth of islands of (1 × 1) in the cross-linked terraces (for example, frame 41) preceded by expansion of the cross-links as a precursor to island growth. The islands continue to grow and new nuclei of the cross-linked (1 × 2) appear by frame 78, followed by the nucleation of new (1 × 2) structures on top of the original surface (frame 98). This cyclical growth of cross-linked (1 × 2) and (1 × 1) continues, apparently *ad infinitum*.

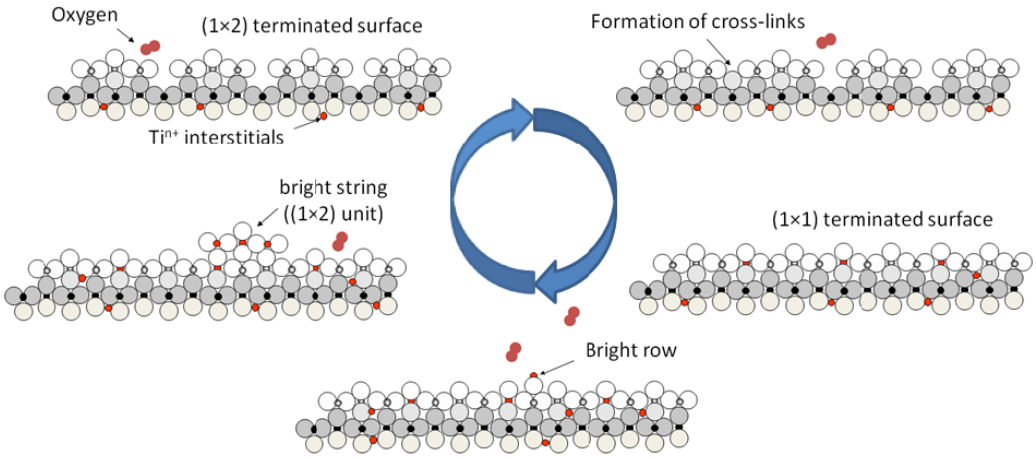

Figure 5. Schematic diagram of the cyclic re-oxidation model in which Ti interstitials diffuse out of the surface to react with ambient oxygen. The cr-(1 × 2) surface initially grows by increasing the number of cross-links until a (1 × 1) termination is reached. Titanium interstitials then lie subsurface awaiting the opportunity to react with an ambient oxygen—first forming bright points and then growing into bright strings which comprise the cr-(1 × 2) surface.

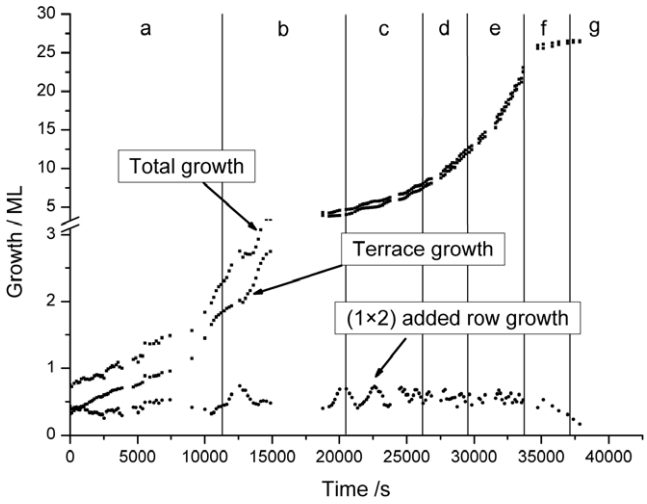

Figure 6. This shows the growth of the (1 × 1) structure and new layers on the cross-linked (1 × 2) surface (formed by treatment and reduction in vacuum) and it is time dependence. There is an oscillation of the amount of the (1 × 2) structure, but every time this forms on a new layer, it is filled in to make the (1 × 1) and every new layer is finally completed in the (1 × 1) structure. However, new growth occurs and so the number of layers (completed in the (1 × 1) structure) increases with time. Within one layer there is a reciprocal relationship between the amount of cr-(1 × 2) and the amount of (1 × 1), as one increases, so the other decreases.

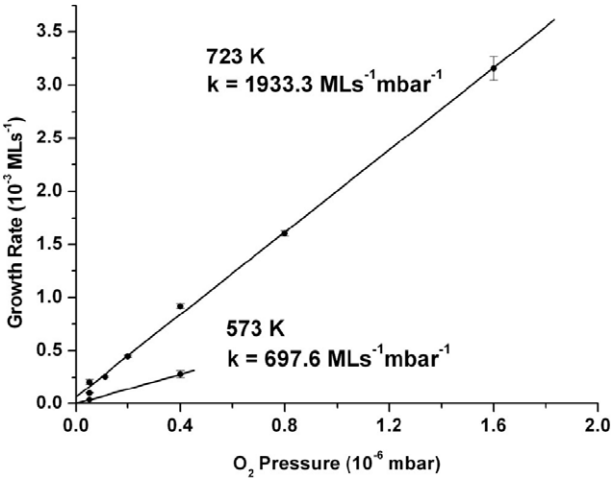

Figure 7. Showing the linear dependence of rate of oxidation of the surface upon oxygen dosing pressure.

for hopping of reduced ions from the surface to beyond the escape depth of the photoelectrons (∼8 ML) [36]. We discuss the kinetics in more detail below.

5. How titania re-oxidizes—by Ti^{3+} out-diffusion

By the use of high temperature STM we have been able to observe the re-oxidation of the titania crystal *in situ* under UHV conditions. An example movie is given in the supplementary information (available at stacks.iop.org/JPhysCM/21/474224), but we have measured this process under a wide range of temperatures, from 573 to 1073 K [16]. At lower temperatures than 573 K the rate of oxidation is very low (see figure 7 below). Figure 4 shows some snapshots from the movie which illustrates the mode of growth of new layers. It occurs by mass transfer to the surface and re-oxidation to produce new layers of titania at the surface. In general the growth occurs by the in-filling of the cross-linked (1 × 2) structure to produce the (1 × 1) surface (for instance, the islands seen growing in frames 53, 66, 78 are of (1 × 1) structure), and then new cross-linked islands grow on top of this. Thus the growth is a cyclic cr-(1 × 2) → (1 × 1) → cr-(1 × 2) mechanism. Note that the (1 × 2) of the Onishi and Iwasawa type is not involved and is not an intermediate in this process. The (1 × 1) grows into the cr-(1 × 2) by in-filling of the empty rows on the surface shown in figure 1(D). Some growth of the cross-links occurs during this process and appears to be intermediate to (1 × 1) formation (compare, for instance, figure 4 frames 5 and 41). Thus the growth proceeds according to the model shown in figure 5, that is, Ti^{3+} interstitials diffuse to the near surface region where they are re-oxidized. In the absence of oxygen the Ti^{3+} interstitials are unlikely to have enough energy to push through to the surface and remain subsurface, although their associated electrons will localize on surface 5-fold sites raising their reactivity considerably. However, when oxygen is in the gas phase, and encounters a Ti^{3+} ion in the surface, reaction occurs and oxidation is initiated, forming the type of small nuclei seen on the (1 × 1) in figure 1(A) and in figure 4, frames 78 and 98. These nuclei act as growth centres for the (1 × 2) phase and grow first in length and then laterally forming a cross-link.

The process is oscillatory in rate, as shown in figure 6, because the oxygen sticking probability on the (1 × 1) surface is smaller than on the cr-(1 × 2). Note also there is locally a counter-correlation between the amount of (1 × 1) and cr-(1 × 2), since, on average, one is growing while the other is shrinking. However, on a macroscopic scale, for example as might be detected by LEED, the surface will be in a mixture of cr-(1 × 2) and (1 × 1). The surface may become terminated by just one of these by appropriate annealing.

We have measured the rates of the growth process at various temperatures and oxygen pressures within the STM to determine the reaction kinetics. We obtain the apparent activation energy for the process, which turns out to be very low, at ∼0.26 ± 0.04 eV/Ti atom. We believe the mechanism of the reaction can be simply written as follows, with the first step being shown as a reversible reaction between bulk (b) and subsurface interstitials (ss),

$$Ti^{3+}_{(b)} \leftrightarrow Ti^{3+}_{(ss)} \quad \text{Step 1} \tag{2}$$

$$Ti^{3+}_{(ss)} + O_{2(g)} + 3e^- \rightarrow TiO_{2(s)} \quad \text{Step 2.} \tag{3}$$

We choose Ti^{3+} as the stable interstitial species dissolved into the bulk generated in accordance with equation (1). If we solve the rate equations using the steady state approximation for the near surface concentration of Ti^{3+} [37] the rate equation becomes

$$R = d(TiO_2)/dt = 27k_2K[Ti^{3+}_b]^4 \cdot P_{O2} \tag{4}$$

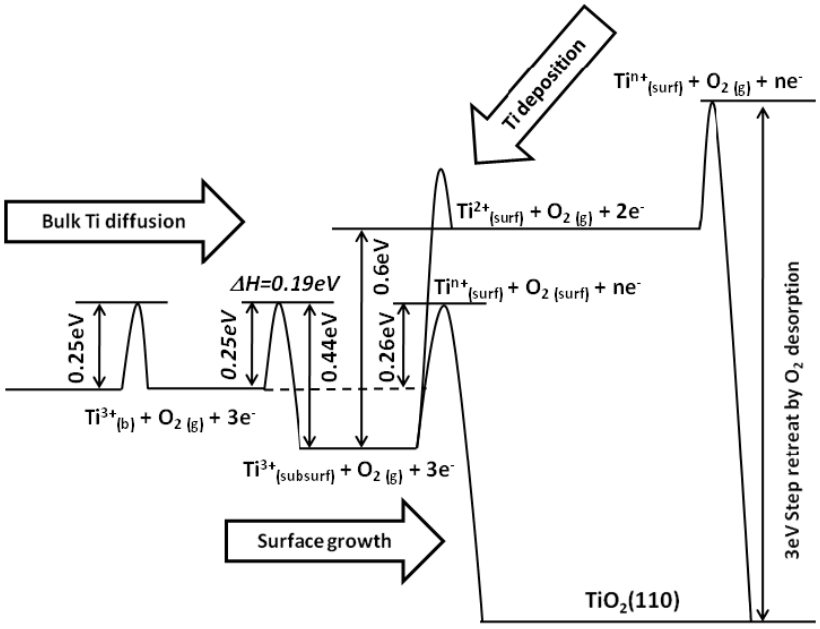

Figure 8. Schematic energy landscape representing oxidation and reduction reactions. Starting from the left we show the 0.25 eV barrier, determined experimentally, for bulk interstitial out-diffusion. The italicized barrier into the subsurface state has not been measured directly but is unlikely to differ significantly from the bulk value. From the far right we show the large 3 eV measured barrier for thermal reduction of the TiO_2(110) surface and concomitant Ti in-diffusion. The upper right hand side pathway shows a schematic barrier for the in-diffusion of Ti deposited on the surface into the subsurface site (which is calculated to be 0.6 eV more stable). We measure a barrier of 0.44 eV for in-diffusion of Ti from surface to bulk which we place at the subsurface bulk step. The Ti in-diffusion process may be viewed as a model of the step following thermal reduction of the surface by desorption of oxygen. In the lower pathway we show the reaction of subsurface interstitial Ti with oxygen to produce surface TiO_2 for which we measure an apparent barrier of 0.26 eV which is the sum of the measured enthalpy ΔH_1 and unknown E_2. We therefore suggest the forward barrier to reaction at the surface E_2 is ≈0.45 eV.

where k_2 is the rate constant for step 2 and K is the equilibrium constant for step 1. The equation is first order in O_2, and we observe exactly that behaviour (figure 7) [37], and is extremely high order in Ti^{3+} concentration in the bulk because of the need for 3 electrons to complete the process of step 2. Note that we believe that the final step of Ti^{3+} out-diffusion from subsurface to create surface TiO_2 is probably enhanced by the presence of oxygen, that is, the barrier to the transfer of Ti^{3+} from a directly subsurface site into the top layer, is lowered by the presence of adsorbed oxygen [28, 29].

Three electrons have been produced by the reduction process of equation (1), and until recently it was not completely clear *exactly* where these electrons are located. As discussed in section 4 above the early calculations predicted they are completely free in the conduction band, while more recent work finds localized states associated with the 5-fold surface Ti and defect sites. The high order power in the Ti^{3+} bulk concentration means an extreme sensitivity of the rate of the oxidation process to the absolute concentration of bulk defects, due principally to the assumed delocalization of the electrons. By considering the electrons to be localized to the defect, a less severe dependence on bulk concentration is predicted which better fits the observed stable oxidation rate over extended periods of time, however it does not impact the value of the activation barrier. The localization of electrons on surface 5-fold Ti in the presence of subsurface Ti provides a natural mechanism for the initial stages of oxygen adsorption. A quantitative study of the stoichiometry dependence of reaction rate would be extremely enlightening in determining the reaction mechanism.

Irrespective of the nature of localization or delocalization we can deduce an activation barrier for the re-oxidation reaction. From measurements of the temperature dependence of the reaction rate we find the *apparent* activation energy for the process to be low at 0.26 eV, which is a combination of the activation energy (E_2) for reaction step 2 and the enthalpy (ΔH_1) for step 1. We can draw the reaction energy profile in figure 8. Many of the energy parameters here need detailed examination and are likely to be sensitive to the degree of bulk reduction, so the diagram is partly conjectural. However, by VT-STM, we have determined $E_2 + \Delta H_1$, as given above, and the step retraction barrier ∼3 eV. It is also known that the activation barrier for Ti bulk diffusion in rutile TiO_2 along the a-axis is ∼0.25 eV [38–40]. However, our surface to bulk diffusion experiments (involving the deposition of Ti from the gas phase onto the TiO_2 surface) yielded 0.44 ± 0.06 eV, which suggests that the surface deposited Ti requires an extra 0.19 eV to surmount the diffusion barrier to the bulk. Recent DFT+U calculations show subsurface interstitial Ti is strongly energetically favoured (0.6 eV through comparison of lowest energy configurations) over surface adsorbed Ti. We therefore feel this enhanced barrier is unlikely to occur in the diffusion of surface Ti to subsurface interstitial sites and is most probable to arise in the step moving from subsurface to bulk. We therefore suggest a model with an energetically shallow trap at the subsurface interstitial site in the Ti diffusion pathway between surface and bulk. The reverse process (out-diffusion

of Ti from the bulk) will populate the subsurface interstitial sites leaving Ti available for reaction. We suggest that the barrier for the diffusion step from bulk to subsurface is likely to be very similar to the value for bulk diffusion which gives $\Delta H_1 \approx 0.19$ eV. The final step in the reaction depends on the presence of adsorbed oxygen. If present a low barrier is found to the creation of new TiO_2 on the surface, if absent the subsurface Ti forms a population in equilibrium with the bulk. Important factors to be recalled from experiment are

(i) thermal reduction of titania is a highly activated process, only occurring at significant rate at very high temperature;
(ii) the energy for the reverse process must be much lower, since we can see it occurring by STM at as low a temperature as 573 K, and that may be dictated by the diffusion of titanium interstitials to the surface, rather than by surface reaction between Ti^{3+} and oxygen;
(iii) in-diffusion of Ti from the surface sees a higher barrier than Ti diffusion in the bulk;
(iv) the enthalpy for step 1 above is exothermic, since, at high temperature surface reduced Ti is lost to the bulk very quickly and there is generally a very low level of surface defects present at elevated temperature, i.e. the reduced Ti prefers to be in the bulk, as dictated by the thermodynamics (the equilibrium level at the surface diminishes with increasing temperature).

Many of these parameters need to be further quantified, but the general scheme for the reaction will be akin to that shown in figure 8, and this also includes the surface Ti^{2+} species identified recently [28, 29].

In conclusion, we can say that much has been learned about the mechanism of the reduction of $TiO_2(110)$ by the application of STM imaging at high temperatures. Titania reduces by thermal oxygen loss at high temperature to leave localized (i.e. Ti^{3+}) and delocalized electrons, and the reduced titania diffuses into the bulk of the crystal. This titania can be recalled to the surface by treatment in very low pressures of oxygen at a significant rate at 573 K. This occurs by re-growth of titania layers in a Volmer–Weber manner, first by in-growth of extra titania within the cross-linked (1×2) structure, to eventually form a complete (1×1). The next layer then initiates as islands of cross-linked (1×2), which grow and fill in once again to (1×1) and so on to continually form new layers of well-ordered titania.

Acknowledgments

The Royal Society/Wolfson foundation is gratefully acknowledged for refurbishment grants for laboratories and computational facilities in Cardiff and Reading. We would like to acknowledge helpful discussions with Dr P A Mulheran and Dr M Nolan.

References

[1] Satterfield C N 1991 *Heterogeneous Catalysis in Industrial Practice* 2nd edn (New York: McGraw-Hill)
[2] Selhofer H 1999 *Vacuum Thin Film* 15
[3] Fujishima A, Hashimoto K and Watanabe T 1999 TiO_2 *Photocatalysis Fundaments and Applications* (Chiyoda-ku: BKC)
[4] Lausmaa J, Ask M, Rolander U and Kasemo B 1988 *Mater. Res. Soc. Symp. Proc.* **110** 647
[5] Diebold U 2003 *Surf. Sci. Rep.* **48** 53
[6] Dubrovinsky L S, Dubrovinskaia N A, Swamy V, Muscat J, Harrison N M, Ahuja R, Holm B and Johansson B 2001 *Nature* **410** 653
[7] An excellent summary is given in Henderson M A 1999 *Surf. Sci.* **419** 174
[8] Huntingdon H B and Sullivan G A 1965 *Phys. Rev. Lett.* **14** 177
[9] Aono M and Hasiguti R R 1993 *Phys. Rev.* B **48** 12406
[10] Bennett R A, Poulston S, Stone P and Bowker M 1999 *Phys. Rev.* B **59** 10341
[11] Rohrer G S, Henrich V E and Bonnell D A 1990 *Science* **250** 1239
[12] Rohrer G S, Henrich V E and Bonnell D A 1992 *Surf. Sci.* **278** 146
[13] Marezio M, Gauzzi A, Licci F and Gilioli E 2000 *Physica* C **338** 1–8
[14] Onishi H and Iwasawa Y 1996 *Phys. Rev. Lett.* **76** 791
[15] Li M, Hebenstreit W, Gross L, Diebold U, Henderson M A, Jennison D R, Schultz P A and Sears M P 1999 *Surf. Sci.* **437** 173
[16] Stone P, Bennett R A and Bowker M 1999 *New J. Phys.* **1** www.njp.org
Bennett R A 2000 *Phys. Chem. Commun.* **3** 9–14
[17] Wendt S, Sprunger P T, Lira E, Madsen G K H, Li Z, Hansen J Ø, Matthiesen J, Blekinge-Rasmussen A, Lægsgaard E, Hammer B and Besenbacher F 2008 *Science* **320** 1755
[18] Bowker M, Poulston S, Bennett R A, Stone P, Jones A H, Haq S and Hollins P 1998 *J. Mol. Catal.* A **131** 185
[19] Zhang L P, Li M and Diebold U 1998 *Surf. Sci.* **412/413** 242
[20] Diebold U, Anderson J F, Ng K O and Vanderbilt D 1996 *Phys. Rev. Lett.* **77** 1322
[21] Asari E and Souda R 2000 *Nucl. Instrum. Methods Phys. Res.* B **161–163** 396
[22] Blanco-Rey M, Abad J, Rogero C, Méndez J, López M F, Martín-Gago J A and de Andrés P L 2006 *Phys. Rev. Lett.* **96** 055502
[23] Blanco-Rey M, Abad J, Rogero C, Méndez J, López M F, Román E, Martín-Gago J A and de Andrés P L 2007 *Phys. Rev.* B **75** 081402
[24] Shibata N, Goto A, Choi S-Y, Mizoguchi T, Findlay S D, Yamamoto T and Ikuhara Y 2008 *Science* **322** 570
[25] Park K T, Pan M H, Meunier V and Plummer E W 2006 *Phys. Rev. Lett.* **96** 226105
[26] Elliott S D and Bates S P 2001 *Phys. Chem. Chem. Phys.* **3** 1954
Elliott S D and Bates S P 2002 *Phys. Rev.* B **65** 245415
[27] Elliott S D and Bates S P 2002 *Phys. Rev.* B **65** 245415
[28] Nolan M, Elliott S D, Mulley J S, Bennett R A, Basham M and Mulheran P A 2008 *Phys. Rev.* B **77** 235424
[29] Mulheran P A, Basham M, Sanville E, Nolan M, Elliott S D and Bennett R A, unpublished results
[30] Bennett R A, Stone P, Price N J and Bowker M 1999 *Phys. Rev. Lett.* **82** 3831
[31] Li M, Hebenstreit W, Diebold U, Tyryshkin A M, Bowman M K, Dunham G G and Henderson M A 2000 *J. Phys. Chem.* B **104** 4944
[32] von Oertzen G U and Gerson A R 2006 *Int. J. Quantum Chem.* **106** 2054
Zhang Y F, Lin W, Li Y, Ding K N and Li J Q 2005 *J. Phys. Chem.* B **109** 19270
Hameeuw K, Cantele G, Ninno D, Trani F and Iadonisi G 2006 *Phys. Status Solidi* a **203** 2219
Cho E, Han S, Ahn H S, Lee K R, Kim S K and Hwang C S 2006 *Phys. Rev.* B **73** 193202

He J and Sinnott S B 2005 *J. Am. Ceram. Soc.* **88** 737
Wang Y, Pillay D and Hwang G S 2004 *Phys. Rev.* B **70** 193410
Rasmussen M D, Molina L M and Hammer B 2004 *J. Chem. Phys.* **120** 988
Paxton A T and Thien-Ng L 1998 *Phys. Rev.* B **57** 1579
[33] Perdew J P 1991 *Electronic Structure of Solids '91* (Berlin: Akademie)
[34] Morgan B J and Watson G W 2007 *Surf. Sci.* **601** 5034
[35] Di Valentin C, Pacchioni G and Selloni A 2006 *Phys. Rev. Lett.* **97** 166803
[36] Mccavish N D 2006 *PhD Thesis* University of Reading
[37] Smith R D, Bennett R A and Bowker M 2002 *Phys. Rev.* B **66** 035409
[38] Lundy T S and Coghlan W A 1973 *J. Physique Coll.* **34** C9-299–302
[39] Radecka M and Rekas M 2002 *J. Eur. Ceram. Soc.* **27** 2001
[40] Lee D-K and Yoo H-I 2006 *Solid State Ion.* **177** 1